



Supplement of

Colored dissolved organic matter (CDOM) alters the seasonal physics and biogeochemistry of the Arctic Mackenzie River plume

Clément Bertin et al.

Correspondence to: Clément Bertin (clement.maxime.bertin@jpl.nasa.gov)

The copyright of individual parts of the supplement might differ from the article licence.

S1. ECCO-Darwin (ED) Southern Beaufort Sea (SBS) configuration

ED-SBS is extracted and modified from the ECCO-Darwin global-ocean biogeochemical state estimate (Carroll et al., 2020, 2022). Simulated ocean and sea-ice dynamics are based on the ECCO LLC270 global configuration (Zhang et al., 2018) and coupled online with the Darwin ocean ecology and biogeochemistry model (Dutkiewicz et al., 2013; Follows et al., 2007). The model simulates the SBS ocean-sea ice-biogeochemical conditions on a curvilinear grid with a horizontal grid spacing ranging from 12 to 15 km. The water column is composed of 46 telescoping vertical levels, ranging from 3-m thick near the surface to 360-m thick near the seafloor (Bertin et al., 2025). The biogeochemical component of the model explicitly simulates the cycling of carbon, nitrogen, phosphorus, silica, iron, and oxygen, transitioning between inorganic, living, and dead organic pools, including the carbonate cycle (Follows et al., 2006). In ED-SBS, four plankton functional types (PFTs) representative of ecosystems in the AO (diatoms, large eukaryotes, and small and large zooplankton) are explicitly simulated, along with phytoplankton Chl concentrations. Initial and boundary conditions for ocean, sea ice, and biogeochemical tracers were derived from the ECCO-Darwin global-ocean biogeochemical estimate (Carroll et al., 2020), except for marine DOC, which were obtained from previous ED-SBS simulations (Bertin et al., 2025).

15 S2. CDOM initial and boundary conditions

We generated CDOM initial conditions in two steps. First, we ran the ED-SBS model for 3 years (2008-2010) with CDOM initial and boundary conditions set to zero and without river discharge. Over the three-year model spin-up, the CDOM field was populated with non-zero values due to ecosystem dynamics (i.e., plankton growth, grazing, and mortality).

For phase two, we extracted CDOM boundary conditions from year-3 of the phase-one simulation described above. A spatial-mean CDOM vertical profile was computed for each open boundary (taken 5 grid cells away from the boundary to prevent zero values), resulting in mean boundary condition profiles for the west and east boundaries for an entire year. We then ran the phase-two simulation for 5 years (2008-2012) with these repeat-year boundary conditions, initial conditions for CDOM set to zero, and included river discharge. We then used the last daily field of the phase-two simulation as CDOM initial conditions in our final simulation. CDOM boundary conditions for the final simulation are the same as in the phase-two simulation.

S3. Comparison metrics

We used 4 comparison metrics to compare retrieved CDOM absorption ($a_{CDOM}[\lambda]$) from simulated CDOM (hereafter X_{mod}) against observations (hereafter X_{obs}): the median (\pm standard deviation), the correlation coefficient (r), the median percent error (MPE) and the unbiased root-mean-square error (MPE). We calculated r, URMSE, and MPE as follows:

$$r = \frac{\sum [(X_{obs} - \overline{X_{obs}}).(X_{mod} - \overline{X_{mod}})]}{\sqrt{\sum (X_{obs} - \overline{X_{obs}})^2.\sum (X_{mod} - \overline{X_{mod}})^2}},$$
(S1)

$$URMSE = \sqrt{\frac{\sum [(X_{mod} - X_{obs}) - (\overline{X_{mod}} - \overline{X_{obs}})]^2}{n}},$$
(S2)

35
$$MPE = Median\left(100. \left| \frac{X_{mod} - X_{obs}}{X_{obs}} \right| \right).$$
 (S3)

The URMSE measures the size of the discrepancies between the simulated and observed values. The MPE is the median of the absolute percentage error and provides insights on the regression model accuracy.

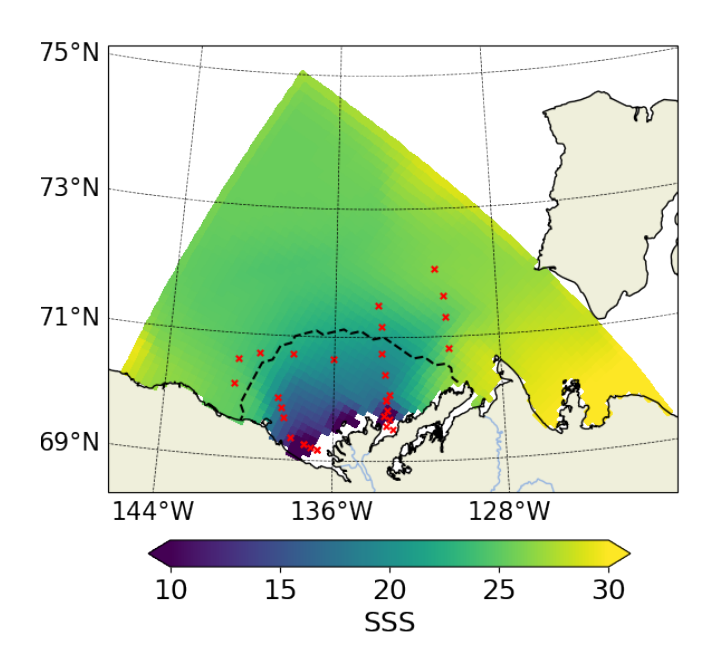


Figure S1. Annual-mean sea-surface salinity simulated by ED-SBS. The black dashed line indicates the 27 isohaline (boundary of the Mackenzie River plume) and red markers show the location of the 2009 Malina campaign stations.

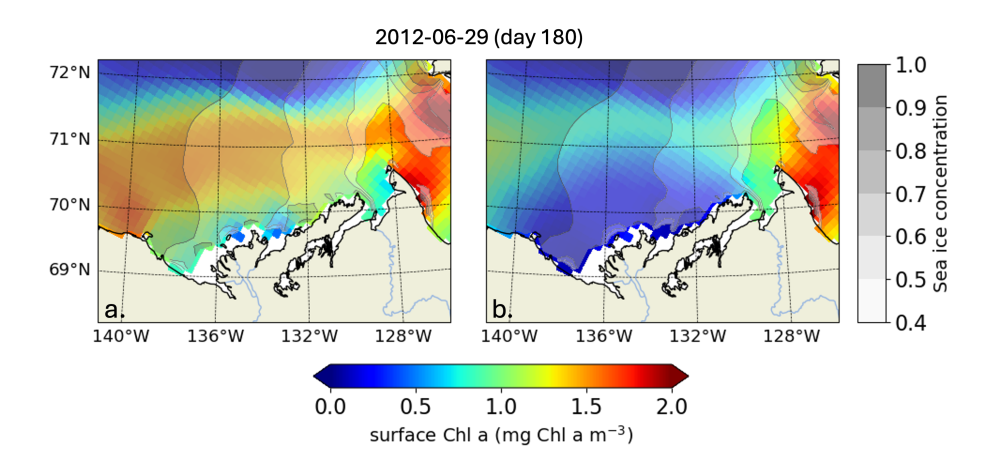


Figure S2. Simulated surface-ocean Chl a (mg Chl a m⁻³) concentration and sea ice concentration for 2012-06-29 (a) without and (b) with the CDOM tracer effect.

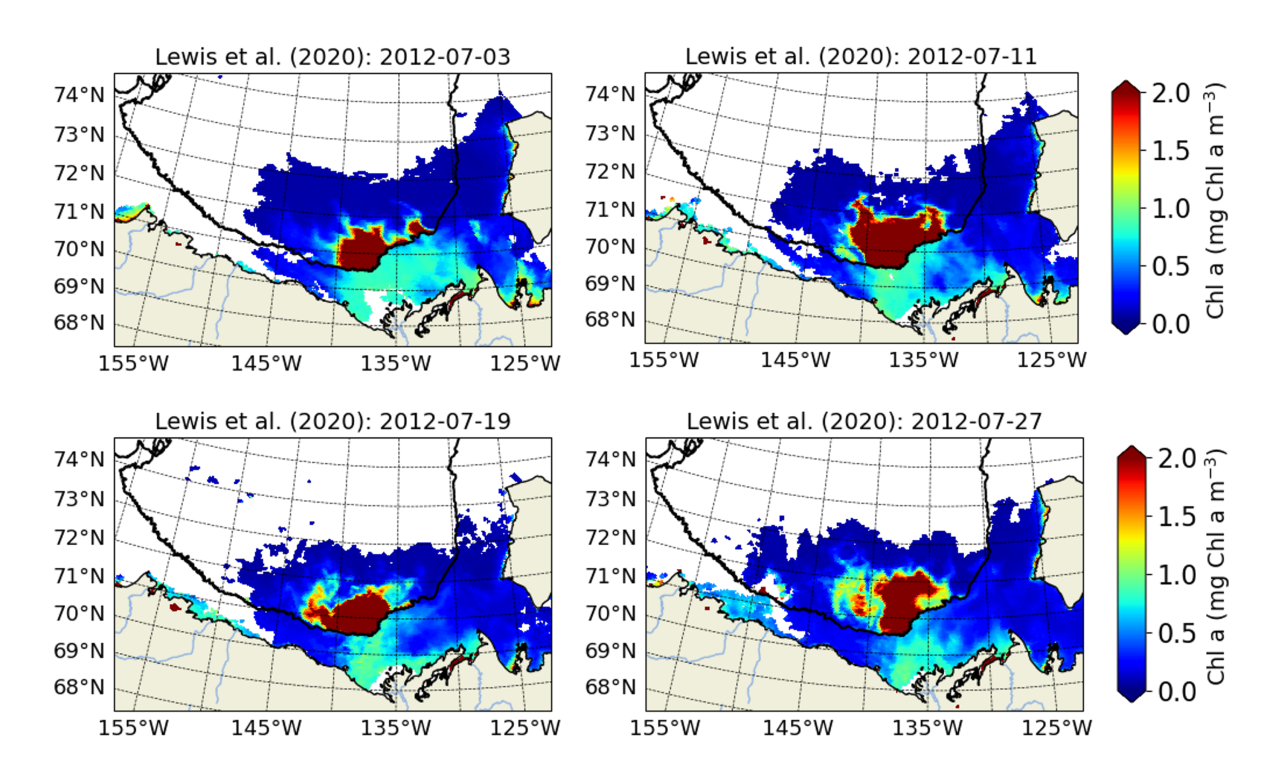


Figure S3. Snapshots of Chl a from Lewis et al. (2020) AOReg.emp satellite observations for 4 days in July 2012.

References

45

50

- 40 Bertin, C., Carroll, D., Menemenlis, D., Dutkiewicz, S., Zhang, H., Schwab, M., Savelli, R., Matsuoka, A., Manizza, M., Miller, C., Bowring, S., Guenet, B., and Le Fouest, V.: Paving the way for improved representation of coupled physical and biogeochemical processes in Arctic River plumes A case study of the Mackenzie Shelf, Permafrost and Periglicial Processes, https://doi.org/10.1002/ppp.2271, 2025.
 - Carroll, D., Menemenlis, D., Adkins, J., Bowman, K., Brix, H., Dutkiewicz, S., Fenty, I., Gierach, M., Hill, C., Jahn, O., Landschützer, P., Lauderdale, J., Liu, J., Manizza, M., Naviaux, J., Rödenbeck, C., Schimel, D., Van der Stocken, T., and Zhang, H.: The ECCO-Darwin data-assimilative global ocean biogeochemistry model: Estimates of seasonal to multidecadal surface ocean pCO₂ and air–sea CO₂ flux, Journal of Advances in Modeling Earth Systems, 12, e2019MS001888, https://doi.org/10.1029/2019MS001888, 2020.
 - Carroll, D., Menemenlis, D., Dutkiewicz, S., Lauderdale, J., Adkins, J., Bowman, K., Brix, H., Fenty, I., Gierach, M., Hill, C., Jahn, O., Landschützer, P., Manizza, M., Mazloff, M., Miller, C., Schimel, D., Verdy, A., Whitt, D., and Zhang, H.: Attribution of Space-Time Variability in Global-Ocean Dissolved Inorganic Carbon, Global Biogeochemical Cycles, 36, e2021GB007162, https://doi.org/10.1029/2021GB007162, 2022.
 - Dutkiewicz, S., Scott, J., and Follows, M.: Winners and losers: Ecological and biogeochemical changes in a warming ocean, Global Biogeochemical Cycles, 27, 463–477, https://doi.org/10.1002/gbc.20042, 2013.
 - Follows, M., Ito, T., and Dutkiewicz, S.: On the solution of the carbonate chemistry system in ocean biogeochemistry models, Ocean Modelling, 12, 290–301, https://doi.org/0.1016/j.ocemod.2005.05.004, 2006.
- Follows, M., Dutkiewicz, S., Grant, S., and Chisholm, S.: Emergent biogeography of microbial communities in a model ocean, science, 315, 1843–1846, https://doi.org/10.1126/science.1138544, 2007.
 - Lewis, K., Van Dijken, G., and Arrigo, K.: Changes in phytoplankton concentration now drive increased Arctic Ocean primary production, Science, 369, 198–202, https://doi.org/10.1126/science.aay8380, 2020.
- Zhang, H., Menemenlis, D., and Fenty, I.: ECCO LLC270 ocean-ice state estimate, Tech. rep., Jet Propulsion Laboratory, California Institute of Technology, Pasadena, CA, 2018.